Two developmental modules establish 3D beak-shape variation in Darwin's finches

Changes in two different developmental modules establish beak shape variation in Darwin's finches

Ricardo Mallarino[a], Anthony Herrel[b], Winston P. Kuo[a, c], B. Rosemary Grant[d], Peter R. Grant[d], and Arhat Abzhanov[a, 1]

[a] *Department of Organismic and Evolutionary Biology, Harvard University, 16 Divinity Avenue, Cambridge, MA 02138, USA,* [b] *Département d'Ecologie et de Gestion de la Biodiversité, 57 rue Cuvier, Case postale 55, 75231, Paris Cedex 5, France,* [d]*Department of Ecology and Evolutionary Biology, Princeton University, Princeton, NJ 08544, USA*

[c] Present address: Department of Developmental Biology, Harvard School of Dental Medicine, 188 Longwood Ave, Boston, MA 02115, USA

[1] To whom correspondence should be addressed. E-mail: abzhanov@fas.harvard.edu

Key Words: Darwin's finches, craniofacial, *TGFβIIr*, *β-catenin*, *Dkk3*, beak morphology

Running title: Modularity in beaks shapes of Darwin's finches

Classification: BIOLOGICAL SCIENCES (evolution, developmental biology)

Abstract

Bird beaks display tremendous variation in shape and size, which is closely associated with the exploitation of multiple ecological niches and likely played a key role in the diversification of thousands of avian species (1). While previous studies described the molecular mechanisms that regulate morphogenesis of the prenasal cartilage (2, 3), which forms the initial beak skeleton, much of the beak diversity in birds depends on variation in the premaxillary bone, which forms later in development and becomes the most prominent functional and structural component of the adult upper beak/jaw (4). Here, we studied the varied beak shapes of Darwin's finches to understand the development and evolution of the premaxillary bone. We show that *TGFβ receptor type II, β-catenin* and *Dickkopf-3*, the top candidate genes from a cDNA microarray screen, are differentially expressed in the developing premaxillary bone in embryos of Darwin's finches, in close correlation with their beak shapes. Furthermore, functional analyses in chick embryos demonstrated that these molecules form a regulatory network shaping the morphology of the premaxillary bone, independently of the network controlling the prenasal cartilage. Our results show that beak morphology is established by two different modules, the prenasal cartilage (during early development) and the premaxillary bone (during late development). We demonstrate that multiple molecules regulate these two modules and can independently alter their growth along different axes, thereby increasing the ability of the beak developmental program to generate variation. This modularity in developmental program may be a general mechanism by which morphological diversity can evolve.

Introduction

Modern evolutionary developmental biology postulates that adaptive morphological changes in adult organisms ultimately originate by altering particular developmental programs (5, 6). Thus, exploring cases in which the developmental pathways responsible for evolutionary changes can be identified and characterized is pivotal to our understanding of the origin of morphological diversity (7-9). In this study, we aimed to understand how changes in developmental controls of a morphological trait may constrain or facilitate diversification. To this end, we focused on unraveling the molecular and developmental mechanisms responsible for patterning the differences in the shapes of avian beaks—which are usually associated with differences in diet and ecological niche—by taking advantage of the natural diversity of beak shapes in the iconic Darwin's finches.

Bird beaks are three-dimensional structures that show a tremendous amount of variation in shape along the depth, width, and length axes. Variation in beak shape has profound impacts in the ability of an organism to survive and reproduce in the wild and, thus, has played a major role in the radiation of thousands of species of birds, one of the most successful classes of vertebrates (1, 10-12). Therefore, its adaptive significance coupled to the extreme levels of diversity observed in nature make this trait ideal for tackling developmental and evolutionary questions about morphological diversification.

Adult beak morphology is determined by the development of two components, the prenasal cartilage (*pnc*; the ethmoid process of the nasal septum) followed by the premaxillary bone (*pmx*) from a separate condensation. Previous studies of *pnc* formation have identified two signaling molecules, *Bmp4* and *CaM*, that regulate early differences in beak morphogenesis (2, 3). Comparable studies of the *pmx* are lacking, and are greatly needed for three reasons. First, it is

the most prominent functional and structural component of the adult bird upper beak/jaw (4). Second, much of beak diversity in birds depends on variation in the *pmx* (4). Third, it is not known if molecules such as *Bmp4* and *CaM* have the same roles at this crucially important stage of development, or the extent to which *pnc* and *pmx* formation are independent modules. Here, we took advantage of the beak shape differences in closely related species of Darwin's finches to understand how variation in the *pmx* is generated and address fundamental questions about the evolution of beak shape diversity.

Darwin's finches (Thraupinae, Passeriformes) of the Galapagos and Cocos Islands comprise a monophyletic group of fourteen closely related species that represent a classic example of adaptive radiation, niche partitioning, and rapid morphological evolution (13-16). In a relatively short period of time, this group has evolved a diversity of bill shapes adapted to exploit specific food items, particularly under conditions of food scarcity (16). Within the monopyletic genus *Geospiza,* the small, medium and large ground finches (*G. fuliginosa*, *G. fortis*, and *G. magnirostris*, respectively), which we refer to as "ground finches" in this article, have evolved a series of deep and broad beaks used to crush seeds. This series of ground finches contrasts with the more elongated and narrow beak shapes used by the large cactus and cactus finches (*G. conirostris* and *G. scandens*) to feed on nectar and pollen (Fig. 1A).

Here, we used a microarray screen results and comparative gene expression analyses in Darwin's finch embryos followed by functional experiments in the chicken model system to determine the molecular and developmental mechanisms responsible for patterning shape differences in the avian beak. Our results show that beak morphology is controlled by two different developmental modules, the *pnc* (during early development) and the *pmx* (during late development). We find that multiple molecules are involved in regulating these two modules and

can independently alter their growth along different axes, thereby increasing the level of morphogenetic variability and potential for evolutionary change.

Results and discussion

During beak development, the *pnc* and the *pmx* condensations are established when the beak primordia form (4). The prenasal cartilage is the first skeletal structure to mineralize and establish species-specific beak shapes during early embryonic development (2, 4). As revealed by the expression pattern of the chondrogenic marker *Col2a1,* at embryonic stage 27 (st. 27), the *pnc* occupies a large portion of the developing upper beak primordia and explains differences in beak shape of the large and medium ground finches at this stage (Fig. 1B). However, its relative contribution to forming overall beak dimensions is significantly diminished by st. 30 (Fig. 1B) (2). At this later stage, the *pmx* condensation begins to expand and it is this structure that will ultimately determine the species-specific differences in adult bird beaks (4).

According to recent mechanical models, the *pmx* is the principal element of the adult bird upper beak responsible for dissipating and distributing forces generated during consumption of hard seeds (17, 18). Correspondingly, our analyses of micro-CT scan data showed that the adult large and medium ground finches have considerably larger *pmx* volumes, relative to their size, than the cactus finches and are, thus, ideal for analysis of variation in the *pmx* (Fig. 1C and Table S1). To determine when the species-specific differences in *pmx* are first established, we examined the expression of alkaline phosphatase, an osteogenic marker, in embryos of five species from the genus *Geospiza* at two critical stages of beak development, st. 27 (E5.5) and st. 30 (E6.5) (2, 3). In the species with the largest *pmx* volume, the large ground finch, alkaline phosphatase was expressed in the condensation of the *pmx* earlier than in any other species (st.

27) indicating that this species undergoes a heterochronic shift in the osteogenesis of this tissue. At the later st. 30, the *pmx* condensation in the large and the medium ground finches expands to occupy most of the upper beak primordium and expresses higher levels of osteogenic markers than size-matched cactus finches (Fig. 1D and Fig. S1). Thus, the results from this analysis showed that differences in adult *pmx* volume in Darwin's finches correlate with the time, strength and place of expression of osteogenic markers during embryonic development.

Previously, we showed that two different molecules, *Bmp4* and *Calmodulin* (*CaM*), regulate growth along different dimensions of the developing beak in Darwin's finches (*depth/width* and *length*, respectively) by patterning the *pnc* element (2, 3). However, our functional tests showed that *Bmp4* and *CaM* do not regulate morphogenesis of the *pmx* (2, 3). To identify genes, in an unbiased manner, that might explain the variation seen in the *pmx* of different species we took advantage of the previously conducted cDNA microarray-based screen in which we directly compared expression of several thousand transcripts from st. 26 upper beak primordia in Darwin's finches (3). We searched for transcripts whose expression levels would correlate with the beak shapes of the large and the medium ground finches as they have considerably deeper and larger *pmx* than cactus finches. We identified three transcripts, *TGFβ receptor type II* (*TGFβIIr*), *β-catenin* and *Dickkopf-3* (*Dkk3*), that were expressed at 12-15 fold higher levels in the large ground finches than in the reference species, the sharp-beaked finch (*G. difficilis*) (Table S2). These three new candidates represented significant developmental pathways and were not housekeeping or ribosomal genes.

TGFβIIr is a serine/threonine protein kinase that upon ligand binding initiates a series of phosporylation events that can lead to the regulation of gene transcription (19). *TGFβIIr*-dependent pathway is important for craniofacial skeletal development in mammals and mutations

in this gene are associated with certain human craniofacial abnormalities (20, 21) but its function in morphogenesis of bird beaks has not been previously reported. *β-catenin* is a subunit of the cadherin protein complex and an integral component in the Wnt signaling pathway (22). While nuclear translocation of *β-catenin* in the osteogenic cells is both required and sufficient for terminal bone cell differentiation, the relationship between its expression level and osteogenic potential is unknown (23). *Dkk3* encodes a secreted protein and is the most divergent member of the *Dkk* family in terms of sequence and function (24). *Dkk3* does not have a reported function in craniofacial or skeletal development and, unlike the other members of the *Dickkopf* family, is not known to regulate Wnt signaling (reviewed in ref. 24).

We observed a striking correlation between adult beak morphology and expression of our three new candidate genes. The three genes were expressed at both higher levels and in broader domains in the large and the medium ground finches than in cactus finches, especially in the large ground finch, in which all three genes were expressed in most of the dorso-distal part of the upper beak primordium that accommodates the *pmx* condensation (Fig. 2). More specifically, at st. 27, the three molecules were strongly expressed throughout most of the beak mesenchyme (except in the prenasal cartilage) in the large ground finches, whereas they were confined to a much smaller region in the size-matched large cactus finches (Fig. 2A). By st. 30, both the large and medium ground finches expressed these molecules at much higher levels and in broader domains in the osteogenic beak mesenchyme than the corresponding large cactus and cactus finches, respectively (Fig. 2B). Notably, *TGFβIIr* and *β-catenin* accumulated in a restricted domain at the distal beak region in the large cactus and cactus finches in contrast to the broad domains for these genes found in the large and medium ground finches (Fig. 2B).

To determine the functional significance of the observed correlations, we used the RCAS replication-competent retroviral vector in the chicken embryo model to mimic the broader and stronger expression patterns of *TGFβIIr, β-catenin,* and *Dkk3* seen in the large and medium ground finches (Fig. 3). Infection with a constitutively active version of the *TGFβ* Type I receptor (RCAS::*Alk5**); with a construct driving expression of the stabilized version of *β-catenin* (RCAS::CA-*β-catenin*); and with a construct carrying the full-length chick homolog (RCAS::*Dkk3*), all led to a significant increase in both beak *depth and length*, relative to the uninfected controls, whereas beak *width* remained relatively unchanged (Fig. 3A, B, D, E, G). Most if not all increase in beak dimensions resulted from changes in the *pmx* element, as revealed by chondrogenic and osteogenic markers (Fig. 3A, B, D, and E). In addition, when we infected chicken embryos with a dominant-negative construct to decrease the levels of *TGFβ* signaling (RCAS::*TGFβr*Δ), we found a significant decrease in beak *depth* and *length,* whereas there was little effect on beak *width* (Fig. 3A, C, G). Likewise, this decrease in *depth* and *length* was a result of the diminished *pmx* dimensions (Fig. 3A, C).

These results differed from the significant increase in beak *depth and width* observed when *Bmp4* signaling is upregulated in the chick embryonic beak with the RCAS::*Bmp4* viral construct (Fig. 3A, F). Previous studies have found that *Bmp4* does not elongate the beak (2, 25). Relative to wing length, the beaks of the large and medium ground finches are proportionally deeper and broader than in the basal sharp-beak finch *G. difficilis* (26-28). Interestingly, their beaks are also longer and thus, *Bmp4* activity alone cannot fully explain morphological variation in this axis (29). Misexpression of the three new candidate molecules did not produce a marked effect on the development of *pnc* (Fig. 3A-E), whereas increased levels of *Bmp4* led to a drastic expansion of the cartilage element and a decrease in *pmx* production and dimensions (Fig. 3A, F)

(2). Therefore, the effect of *Bmp4* upregulation on the final beak shape must be indirect, perhaps by providing extensive matrix support for the nascent *pmx* later in development when expression of this gene is shut off. Together, these data suggest that *TGFβIIr*, *β-catenin*, and *Dkk3,* in good correlation with their spatial and temporal expression, act by positively regulating the size of the *pmx*, thereby specifying the final beak morphology in the large and medium ground finches (2).

Since *TGFβIIr, β-catenin, Dkk3* displayed largely overlapping domains of expression in the beak primordia and were co-expressed in many of the same mesenchymal cells (Fig. S2), they could potentially be regulating each other's expression during beak development. To investigate this possibility, we analyzed the effects of misexpressing each candidate molecule on other candidate genes as well as on *Bmp4* (Fig. 4A-D). We found that upregulation of the *TGFβIIr*-dependent pathway or *β-catenin* caused a strong upregulation of *Dkk3* expression (Fig. 4A). Conversely, downregulation of the *TGFβIIr* pathway produced a decrease in the expression of *Dkk3,* suggesting that *Dkk3* is downstream of both *TGFβIIr* and *β-catenin* pathways (Fig. 4A). Furthermore, our analysis also demonstrated that *β-catenin*, *TGFβIIr*, *CaM,* and *Bmp4* do not regulate each other's expression (Fig. 4B-D) suggesting that all these molecules can regulate beak development independently by altering different axes of growth.

In summary, *Bmp4* and *CaM* play important roles in the early expansion of the *pnc* skeleton in ground and cactus finches, respectively (2, 3). This sets the stage, likely indirectly, for the later morphogenesis of the *pmx*, which is patterned through the coordinated action of a small network of unrelated but interacting regulatory molecules, *TGFβIIr*, *β-catenin*, and *Dkk3* (Fig. 4E) (2, 3). This pattern is consistent with previous heritability studies of single populations, which demonstrated the polygenic nature of beak shapes in Darwin's finches (16, 29). These three new candidates not only contribute to beak morphogenesis but their expression and

functions help to comprehensively explain the observed morphological differences among the species we studied. For example, during the evolution of the extremely specialized "grosbeak" shape in the large ground finch, its depth increased by 92% relative to the basal condition in *G. difficilis* and *Bmp4* with all the new candidates contribute to this depth increase. However, its length also increased, albeit much more slowly, by about 30%, and this change cannot be explained by action of *Bmp4* alone, which does not regulate growth along this axis (2). Likewise, beak width increased by 87% and such increase cannot be explained by the activity of bone-specific genes alone (Fig. 5).

Taken together, our results show how changes in expression of multiple molecules regulating the formation of two distinct developmental modules, the *pnc* (in early development) and the *pmx* (in late development), can generate the morphological variation observed in the beaks of Darwin's finches. Our experiments revealed that the three axes of beak growth –depth, length, and width- are regulated differently at these two stages of development, thereby enhancing the ability of the beak developmental program to generate variation on which natural selection can act. Since all modern birds share the same overall beak skeletal structure, while differing remarkably in size, proportions and curvature, our results provide a general developmental framework for understanding how the great diversity of beak shapes observed in nature is brought about developmentally. We suggest that the evolution of beak diversity has involved coordinated changes in multiple tissues and pathways. This is an example of how changes in the modular developmental program of an adaptive trait may facilitate diversification and may represent a general mechanism by which morphological diversity can evolve.

Materials and methods

Darwin's Finches embryo collection and preparation.

Embryos of Darwin's finches were collected according to regulations established by the Galapagos National Park using methods described in detail elsewhere (30). A total of 33 embryos were analyzed: *Geospiza magnirostris* (st. 27, n = 3; st. 30, n = 3), *G. fortis* (st. 27, n = 4; st. 30, n = 5), *G. fuliginosa* (st. 27, n = 3; st. 30, n = 3), *G. scandens* (st. 27, n = 3; st. 30, n = 5), *G. conirostris* (st. 27, n = 2; st. 30, n = 2).

In situ hybridizations and Immunohistochemistry

In situ hybridizations were performed as described before (30) using the *in situ* hybridization antisense probes for chicken. For immunohistochemistry, sections were blocked with 3% Bovine Serum Albumin (BSA) in PBS containing 0.1% Triton-X 100 for 1 hour, incubated overnight with primary antibody at 4 ºC, washed in PBS, incubated for 1hr with secondary antibody, and washed with PBS. Immunostaining was performed using anti-*TGFβIIr* (sc-400; Santa Cruz), anti-*TGFβ1, β2, β3* (sc-146, sc-90, sc-82, respectively; Santa Cruz), anti-*β-catenin* (610153; BD Transduction Laboratories), and anti-*Dkk3* (kindly provided by Dr. Christof Niehrs). Antibodies were used at dilutions of 1:50 – 1:200. Reactions were visualized with Alexa Dye conjugated secondary antibodies (Molecular Probes) at 1:500 dilution in 3% BSA/PBS/Triton-X 100. For controls, sections were incubated with PBS instead of primary antibodies but no specific cellular staining was observed.

Alkaline phosphatase. Embryos were blocked with 3% Bovine Serum Albumin (BSA) in PBS containing 0.1% Triton-X 100 for 1 hour and incubated with an AP-conjugated secondary

antibody (Jackson ImmunoResearch). The signal was detected using a combination of NBT and BCIP to produce a purple precipitate.

Functional experiments in chick embryos

CDNA fragments containing a constitutively active form of the *TGFβIr* (*Alk-5*) (Addgene plasmid 14833) (31), a dominant negative form of *TGFβIIr* (Addgene plasmid 1176) (32), and the entire coding region of the chicken *Dkk3* (gift of Dr. Chris Niehrs) were cloned into the *SLAX-13* vector and then subcloned into *RCAS(BP)A* using methods described before (33). RCAS::CA-*B-catenin* and RCAS::*Bmp4* constructs have been described previously (34, 35). Viruses were harvested, concentrated, and titered using methods described before (33). Fertilized eggs were obtained from SPAFAS (Norwich, CT), incubated at 37 ºC, and staged according to Hamburger and Hamilton (36). Frontal nasal processes were infected at st. 24 and embryos were collected at stage 36 Embryos were fixed overnight in 4% paraformaldehyde, washed in PBS, stained with SYBR-safe (Invitrogen) and photographed under UV light under a Zeiss Discovery v8 Stereoscope (Carl Zeiss Inc). Frontal and lateral images were taken for each head, and measurements of different upper beak parameters were recorded using the Axiovision 4.6.3 software (Carl Zeiss Inc). Measurements were obtained in triplicate as follows: *Length*: from anterior part of nostril to posterior tip of egg tooth; *Depth*: perpendicular line passing through the anterior part of the nostril; *Width*: distance between the nostrils. The extent of viral infection was assayed by *in situ* hybridization with a viral specific probe (*RSCH*). Upregulation of *β-catenin* and of *Dkk3* was monitored using the antibodies and *in situ* hybridization probe described above.

(micro) Computed Tomography (CT) scans

Darwin's finches specimens were scanned at the Harvard CNS facility using an X-Tek XRA-002 micro-CT imaging system set at 75 kV. Specimens were mounted on a rotating table and a series of 3142 projections of 2000 by 2000 pixels covering 360 degrees was recorded. Volume and surface rendering was performed using AMIRA 5.0 (64-bit version, Computer Systems Mercury) for all specimens and the volume of the upper beak was extracted. As species differ in their body and head size rendering comparisons across species difficult, we calculated a multivariate indicator of overall size. To do so we used the Log_{10} transformed wing chord length, tarsus length, head length, head width and head depth for each specimen as input into a factor analysis which is resulted in a single new factor hereafter referred to as 'size'. Log_{10} transformed beak volume was then regressed against 'size' and unstandardized residuals were extracted for comparison.

Darwin's finches microarray screen

Details of the microarray production and data analysis are described elsewhere (3) and in the Supplementary Information.

Acknowledgements

We thank M. Manceau and J. Gros for technical assistance and all the field assistants and participants of the field collecting trips—J. Chavez, G. Castaneda, O. Perez, F. Brown, A. Aitkhozhina, M. Gavilanes, M. Paez, F. Moscoso, G. Granja, C. Clabaut, J. Gee, K. Petren, J. Podos and S. Kleindorfer- for their help and advice. C. Tabin, M. Brenner, M. Manceau, and H. Hoekstra provided comments and discussion on the manuscript. The Charles Darwin Research Station on Santa Cruz Island and The Galapagos National Park provided logistical support and

help with permits. A.A. and R.M. were supported by a grant from the NSF (10B-0616127). R.M. was also supported in part by a Doctoral Dissertation Improvement Grant from the NSF (0909695).

References

1. Gill FB (2007) *Ornithology* (W. H. Freeman and Company, New York, NY)
2. Abzhanov A, Protas M, Grant BR, Grant PR, & Tabin CJ (2004) Bmp4 and morphological variation of beaks in Darwin's finches. *Science* 305(5689):1462-1465.
3. Abzhanov A*, et al.* (2006) The calmodulin pathway and evolution of elongated beak morphology in Darwin's finches. *Nature* 442(7102):563-567.
4. Hanken J & Hall BK (1993) *The Skull* (University of Chicago Press, Chicago).
5. Carroll SB (2008) Evo-devo and an expanding evolutionary synthesis: a genetic theory of morphological evolution. *Cell* 134(1):25-36.
6. Kirschner M & Gerhart J (2005) *The plausibility of life : resolving Darwin's dilemma* (Yale University Press, New Haven).
7. Averof M & Patel NH (1997) Crustacean appendage evolution associated with changes in Hox gene expression. *Nature* 388(6643):682-686.
8. Cohn MJ & Tickle C (1999) Developmental basis of limblessness and axial patterning in snakes. *Nature* 399(6735):474-479.
9. Shapiro MD*, et al.* (2004) Genetic and developmental basis of evolutionary pelvic reduction in threespine sticklebacks. *Nature* 428(6984):717-723.
10. Amadon D (1950) The Hawaiian Honeycreepers. *Bulletin of the American Museum of Natural History* 95(151).
11. Herrel A, Speck T, & Rowe NP (2006) *Ecology and biomechanics : a mechanical approach to the ecology of animals and plants* (CRC/Taylor & Francis, Boca Raton).
12. McCormack JE & Smith TB (2008) Niche expansion leads to small-scale adaptive divergence along an elevation gradient in a medium-sized passerine bird. *Proc Biol Sci* 275(1647):2155-2164.
13. Darwin C (1839) *Journal of researches into the geology and natural history of the various countries visited by H. M. S. Beagle, under the command of Captain FitzRoy, R. N., from 1832 to 1836* (H. Colburn, London,).
14. Lack DL (1947) *Darwin's finches* (University Press, Cambridge).
15. Bowman RI (1961) *Morphological differentiation and adaptation in the Galápagos finches* (University of California Press, Berkeley,).
16. Grant PR (1999) *Ecology and evolution of Darwin's finches* (Princeton University Press, Princeton, N.J.).
17. Herrel A, Podos J, Huber SK, & Hendry AP (2005) Evolution of bite force in Darwin's finches: a key role for head width. *Journal of Evolutionary Biology* 18(3):669-675.
18. Soons J*, et al.* (Mechanical stress, fracture risk and beak evolution in Darwin's ground finches (Geospiza). *Philos Trans R Soc Lond B Biol Sci* 365(1543):1093-1098.
19. Shi Y & Massague J (2003) Mechanisms of TGF-beta signaling from cell membrane to the nucleus. *Cell* 113(6):685-700.

20. Ito Y*, et al.* (2003) Conditional inactivation of Tgfbr2 in cranial neural crest causes cleft palate and calvaria defects. *Development* 130(21):5269-5280.
21. Loeys BL*, et al.* (2006) Aneurysm syndromes caused by mutations in the TGF-beta receptor. *N Engl J Med* 355(8):788-798.
22. Hartmann C (2006) A Wnt canon orchestrating osteoblastogenesis. *Trends Cell Biol* 16(3):151-158.
23. Milat F & Ng KW (2009) Is Wnt signalling the final common pathway leading to bone formation? *Mol Cell Endocrinol* 310(1-2):52-62.
24. Niehrs C (2006) Function and biological roles of the Dickkopf family of Wnt modulators. *Oncogene* 25(57):7469-7481.
25. Wu P, Jiang TX, Suksaweang S, Widelitz RB, & Chuong CM (2004) Molecular shaping of the beak. *Science* 305(5689):1465-1466.
26. Grant PR, Abbott, I., Schluter, D., Curry, R. L., Abbott, L. K. (1985) Variation in the size and shape of Darwin's finches. *Biological Journal of the Linnean Society* 25(1):1-104.
27. Petren K, Grant, B. R., Grant, P. R. (1999) A phylogeny of Darwin's finches based on microsatellite DNA length variation. *Proceedings of the Royal Society B: Biological Sciences* 266(1417): 321-329.
28. Petren K, Grant PR, Grant BR, & Keller LF (2005) Comparative landscape genetics and the adaptive radiation of Darwin's finches: the role of peripheral isolation. *Mol Ecol* 14(10):2943-2957.
29. Grant PR & Grant BR (2008) *How and why species multiply : the radiation of Darwin's finches* (Princeton University Press, Princeton).
30. Abzhanov A (2009) Darwin's Finches: Analysis of Beak Morphological Changes During Evolution. *CSH Protoc* 2009(3):pdb emo119.
31. Feng XH & Derynck R (1996) Ligand-independent activation of transforming growth factor (TGF) beta signaling pathways by heteromeric cytoplasmic domains of TGF-beta receptors. *J Biol Chem* 271(22):13123-13129.
32. Wrana JL*, et al.* (1992) TGF beta signals through a heteromeric protein kinase receptor complex. *Cell* 71(6):1003-1014.
33. Logan M & Tabin C (1998) Targeted gene misexpression in chick limb buds using avian replication-competent retroviruses. *Methods* 14(4):407-420.
34. Duprez D*, et al.* (1996) Overexpression of BMP-2 and BMP-4 alters the size and shape of developing skeletal elements in the chick limb. *Mech Dev* 57(2):145-157.
35. Kengaku M*, et al.* (1998) Distinct WNT pathways regulating AER formation and dorsoventral polarity in the chick limb bud. *Science* 280(5367):1274-1277.
36. Hamburger V & Hamilton HL (1951) A Series of Normal Stages in the Development of the Chick Embryo. *Journal of Morphology* 88(1):49-92.

Figures

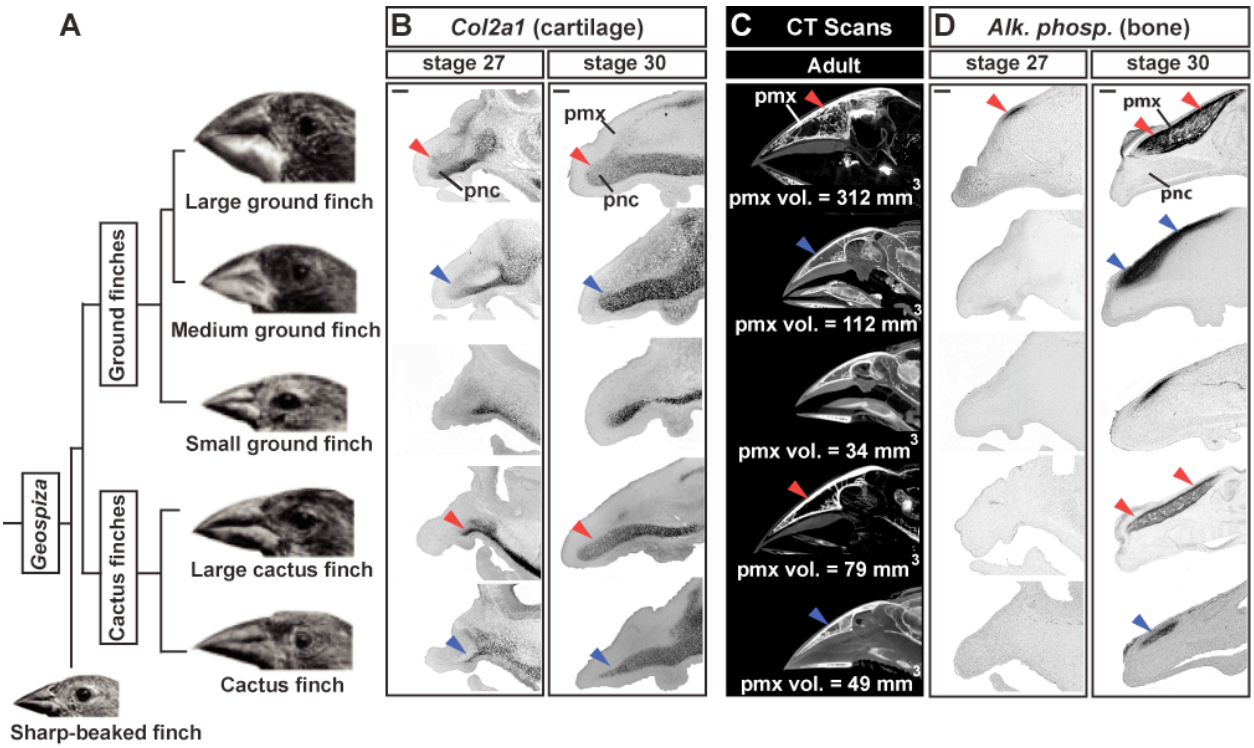

Fig 1. Contribution of the different skeletal structures to beak variation in Darwin's finches. (A) Ground finches (*G. fuliginosa*, *G. fortis* and *G. magnirostris*) have deep beaks used to crack seeds. In contrast, cactus finches (*G. scandens* and *G. conirostris*) use their elongated beaks to feed on pollen and nectar from flowers. (B) At stage (st.) 27 the prenasal cartilage (*pnc*) condensation, labeled with *Col2a1,* occupies a significant portion of the beak primordia in the large and medium ground finches, where is patterned by *Bmp4* and *Calmodulin* (*CaM*). By st. 30, the *pnc*, labeled with *Col2a1*, occupies a smaller proportion of the beak relative to the developing premaxillary bone (*pmx*) and its role in generating species-specific beak morphologies decreases. (C) Micro-Computer Tomography (CT) scans indicate that interspecific variation in Darwin's finches is caused mainly by differences in the amount of the *pmx*. Adults large and medium ground finches have larger *pmx* volumes than their size-matched large cactus and cactus finches, respectively. (D) These differences in adult *pmx* volume correlate with the

expression of the osteogenic marker alkaline phosphatase (*Alk. Phosp*.) during embryonic development. In the large ground finch, alkaline phosphatase is expressed in the condensation of the *pmx* earlier than in any other species (st. 27). By st. 30, this marker is expressed at higher levels and in larger domains in the large and medium ground finches than in the size-matched large cactus and cactus finches, respectively. Arrow colors in B-D indicate species that have comparable body sizes but differ in beak morphology. Scale bar: 0.15 mm (stage 27) and 0.2 mm (stage 30) in (B); 0.2 mm in (C). Molecular tree from ref 27. Abbreviations: *pmx*, premaxillary bone; *pnc*, prenasal cartilage. *Pmx* volumes are corrected for body size.

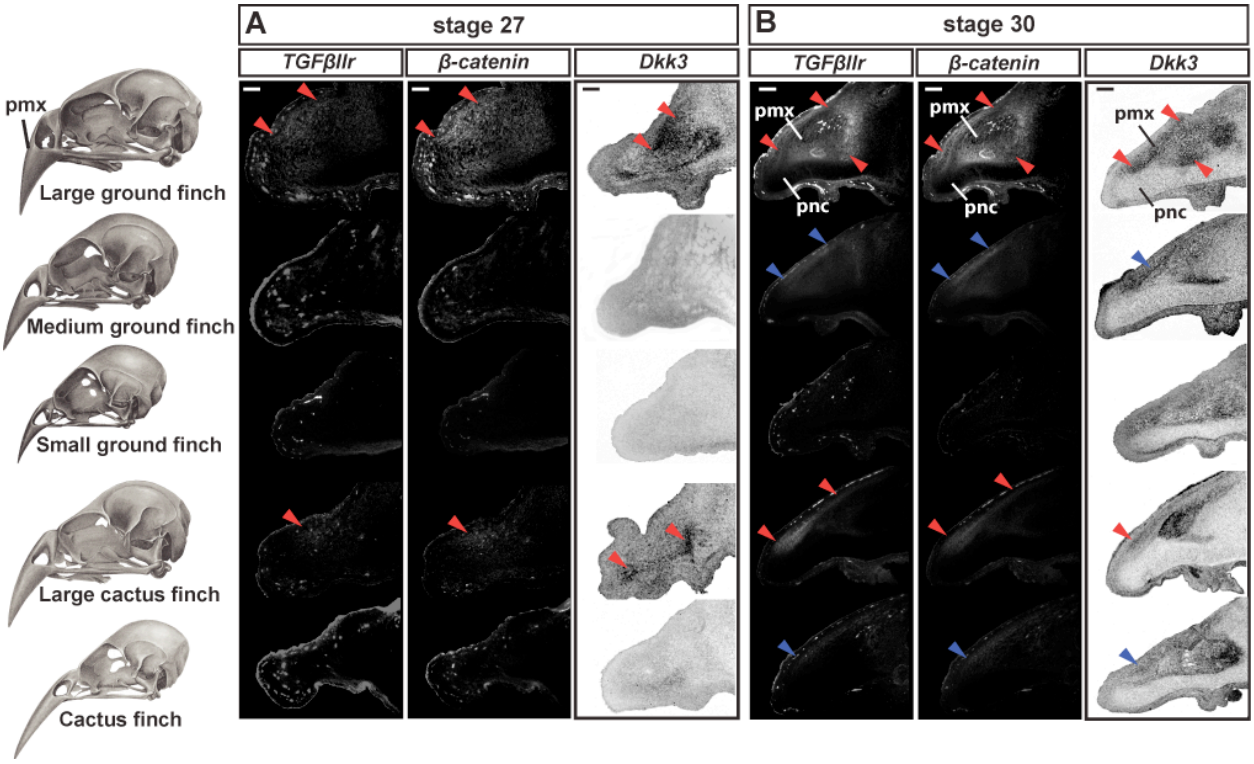

Fig. 2. Variation in the premaxillary bone (*pmx*) in *Geospiza* correlates with the expression of *TGFβIIr, β-catenin* and *Dkk3.* (A) In the large ground finch, the skeletogenic condensation for the *pmx* appears earlier (st. 27) than in the other species showing a strong correlation with the earlier and broader expression of *TGFβIIr, β-catenin,* and *Dkk3.* At st. 30, the large and medium

ground finches have high expression levels of *TGFβIIr, β-catenin* and *Dkk3* in strong correlation with the volume of the developing *pmx*. Arrow colors in A and B indicate species that have comparable body sizes but differ in beak morphology. Scale bar: 0.1 mm in (A) and 0.2 mm in (B). Images of skulls are from ref. 15, with permission from the author. Abbreviations: *pmx*, premaxillary bone; *pnc*, prenasal cartilage

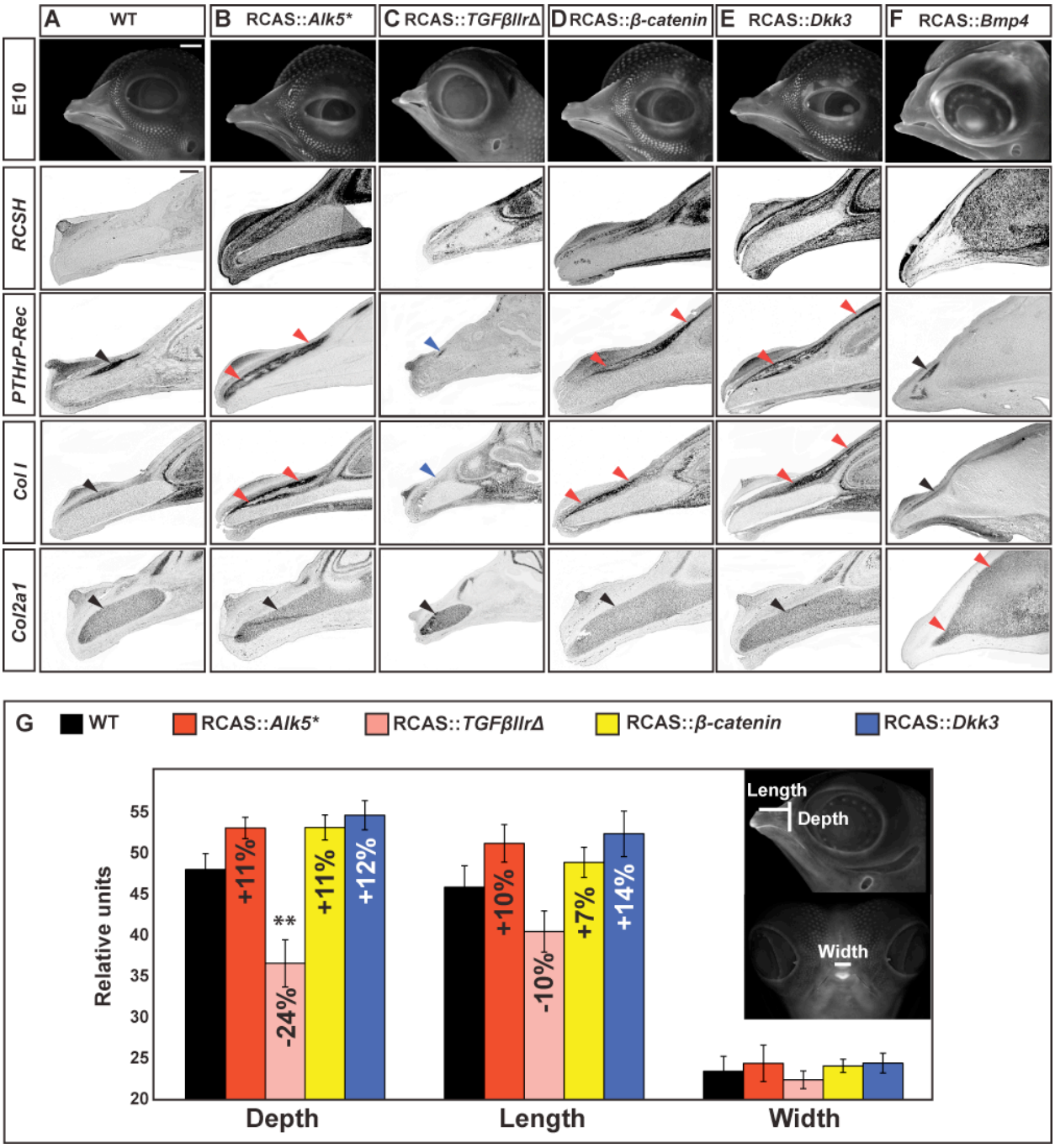

Fig. 3. Functional analysis of *TGFβIIr*, *β-catenin,* and *Dkk3* in the chicken model system.

(A- F) Ultraviolet pictures of embryonic day 11 (HH st. 37) (A) wildtype chicken embryos and embryos infected with (B) RCAS::*Alk5**, (C) RCAS::*TGFβr*Δ, (D) RCAS::CA-*β-catenin,* (E) RCAS::*Dkk3,* and (F) RCAS::*Bmp4* constructs. We used RSCH, *PTHrP-Rec*, *Col I* and *Col II*, probes to reveal RCAS infection (RSCH), early osteoblasts (*PTHrP-Rec*), (overall bone (*Col I*)

and chondrocytes (*Col2a1*). Blue arrows indicate lower expression relative to wildtype specimens, red arrows indicate higher expression, and black arrows indicate no change. (G) Histogram showing beak variation in wildtype and RCAS-infected chicken embryos. Embryos infected with RCAS::*Alk5*,* RCAS::*TGFβrΔ*, RCAS::CA-*β-catenin,* and RCAS::*Dkk3* showed a significant change in their *depth* and their *length* relative to wild-type controls whereas the *width* remained unchanged (RCAS::*Alk5**: $n = 8$; $\mu_{depth} = 53.12 \pm 1.2$ ($\pm$ s.d); $\mu_{length} = 51.39 \pm 2.06$; $\mu_{width} = 24.05 \pm 2.03$; $P_{depth} = 7.65 \times 10^{-6}$; $P_{length} = 0.0002$; $P_{width} = 0.53$; RCAS::*TGFβrΔ*: $n = 9$; $\mu_{depth} = 36.49 \pm 2.85$; $\mu_{length} = 40.35 \pm 4.49$; $\mu_{width} = 22.43 \pm 1.07$; $P_{depth} = 3.32 \times 10^{-8}$; $P_{length} = 0.007$; $P_{width} = 0.1663$; RCAS::CA-*β-catenin*: $n = 9$; $\mu_{depth} = 52.92 \pm 1.51$; $\mu_{length} = 48.91 \pm 1.86$; $\mu_{width} = 24.11 \pm 0.82$; $P_{depth} = 1.21 \times 10^{-5}$; $P_{length} = 0.0079$; $P_{width} = 0.3364$; RCAS::*Dkk3*: $n = 15$; $\mu_{depth} = 54.39 \pm 1.76$; $\mu_{length} = 52.15 \pm 2.76$; $\mu_{width} = 24.43 \pm 1.19$; $P_{depth} = 2.02 \times 10^{-8}$; $P_{length} = 1.04 \times 10^{-5}$; $P_{width} = 0.1239$; WT: n = 9; $\mu_{depth} = 47.8 \pm 1.93$; $\mu_{length} = 45.6 \pm 2.59$; $\mu_{width} = 23.44 \pm 1.83$). Scale bar: 200 mm in whole-head images and 0.4 mm in sections (A-F).

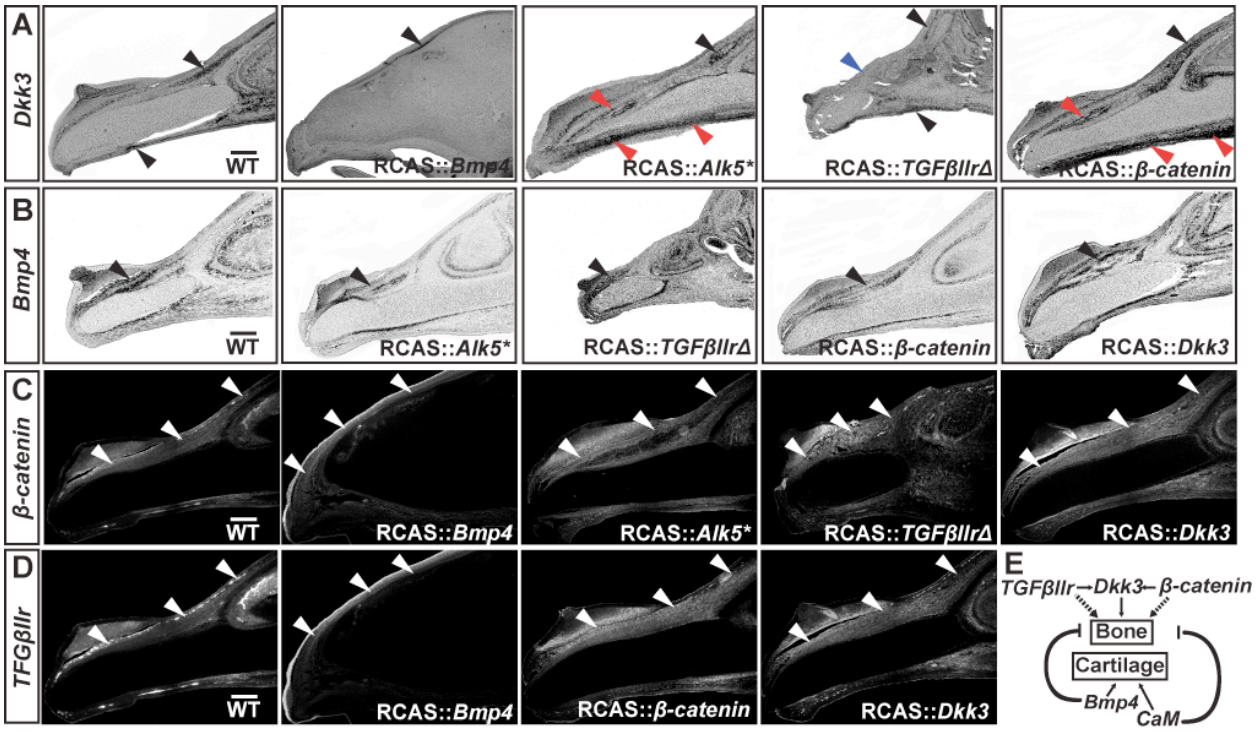

Fig. 4. Interaction of genes regulating beak development. (A) Increasing levels of *Bmp4* didn't have an effect on the expression of *Dkk3* relative to uninfected wildtype controls. However, upregulation of the *TGFβ* pathway and of *β-catenin* led to more cells expressing *Dkk3* relative to uninfected embryos. Conversely, downregulation of the *TGFβ* pathway caused a decrease in the number of cells expressing *Dkk3*. (B) Neither alterations in the *TGFβ* signaling pathway nor upregulation of *β-catenin* or *Dkk3* caused changes in the expression of *Bmp4* relative to wildtype embryos. (C) Similarly, alteration of *TGFβ* signaling and upregulation of *Bmp4* and *Dkk3* did not have an effect in the expression of *β-catenin* relative to wildtype embryos. (D) Likewise, upregulation of *β-catenin, Dkk3 or Bmp4* did not have an effect in the expression of *TGFβIIr* compared to wildtype embryos. (E) *Bmp4* and *CaM* act independently to alter the growth of the prenasal cartilage whereas *TGFβIIr*, *β-catenin,* and *Dkk3* regulate the premaxillary bone. Scale bar: 0.4 mm in (A) and (B) and 0.2 mm in (C) and (D).

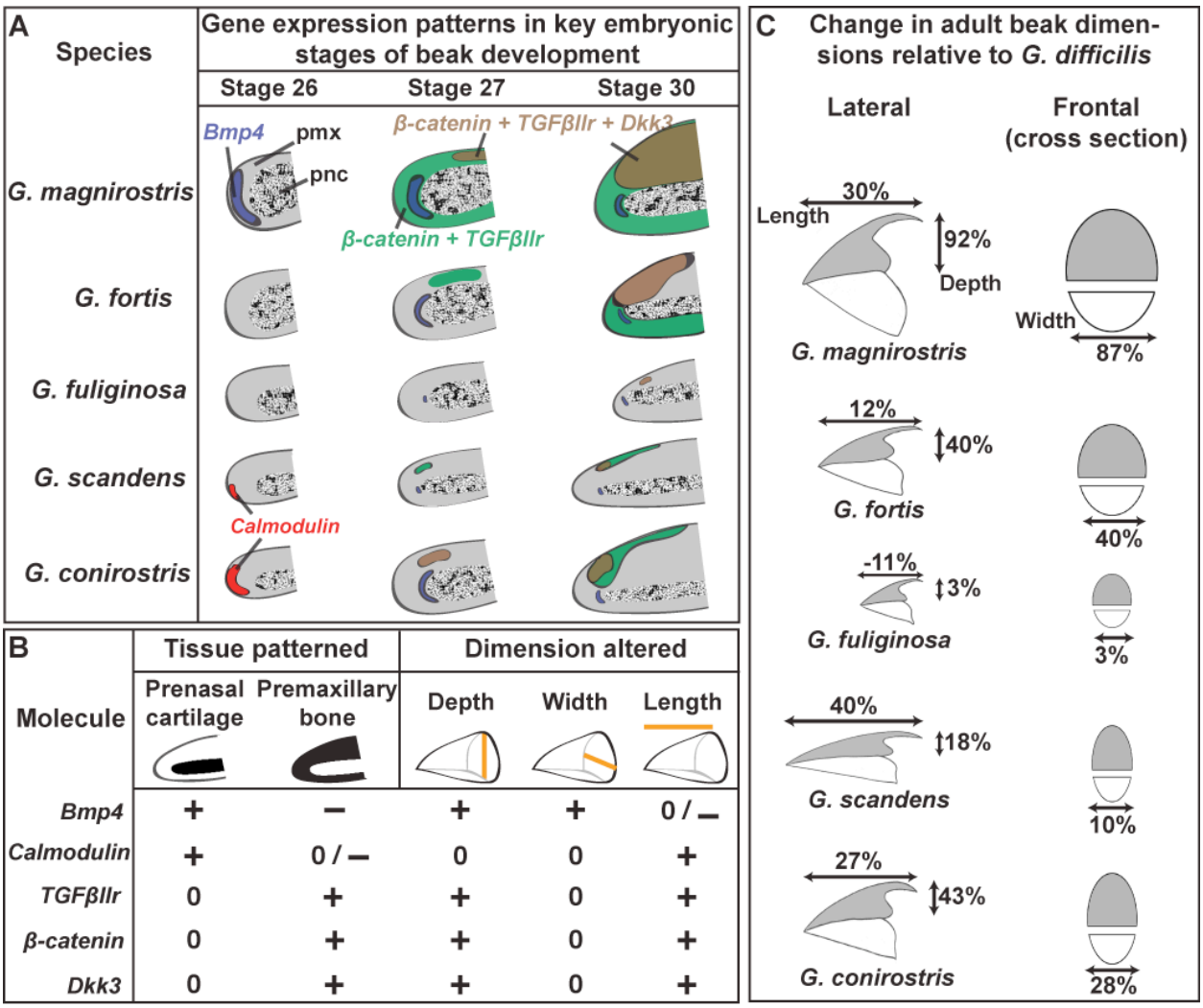

Fig. 5. The distinct beak morphologies in *Geospiza* are generated by differences in the strength, time, and place of expression of the molecules involved in beak development. (A) Species with deep beaks, such as the large ground finch, *G. magnirostris*, express higher levels of *Bmp4*, *TGFβIIr*, *β-catenin,* and *Dkk3,* whereas species with elongated beaks, such as the large cactus finch, *G. conirostris*, express higher levels of *CaM.* (B) Through their action on different skeletal tissues, the different molecules modify independent dimensions of growth and thereby, pattern the species-specific beak morphologies of Darwin's finches. (C) The beak of the sharp-beaked finch, *G. difficilis,* represents a basal morphology for *Geospiza* (27, 28). Expression and function of *Bmp4*, *CaM, TGFβIIr*, *β-catenin,* and *Dkk3*, explain changes in the different beaks

dimensions of the more derived species. Symbols used: + (positive effect); **0** (no effect); **-** (negative effect). Abbreviations: *pmx*, premaxillary bone; *pnc*, prenasal cartilage. Measurements in **c** were taken from ref. 32, corrected for wing length, and correspond to averages from males that were collected in the islands where we obtained our samples. For the *G. difficilis* reference, the analysis was performed with different populations (26) and since all the results showed the same trend we used the population from Wolf because it represents one of the most basal populations (28).